Material Parameters Specifying the Delayed Retardation Phenomenon of Fatigue Crack Growth After a Single Application of Overload

Kohichi Tanaka
Technological University of Nagaoka, Japan
Saburo Matsuoka
National Research Institute for Metals, Japan

A pulse load applied to a fatigue crack propagation under constant amplitude loading results in a delayed retardation phenomenon in the subsequent crack growth. Matsuoka and Tanaka [1, 2] have found that this behavior is specified by two parameters m and ω_B/ω_D, where m is the exponent of the Paris equation under constant amplitude loading and ω_D and ω_B are the overload-affected-zone size and the crack distance at the minimum rate of crack propagation (inflection point), respectively. In the present report, the parameters characterizing the retardation phenomena for various steels and alloys were compiled from previous studies [1 - 6], and the results were analyzed according to a generalized conception using the cyclic J-integral [7 - 10].

DELAYED RETARDATION CURVE

Sometimes a disturbance imposed on a physical phenomenon reveals the nature of the phenomenon, which may not be realized explicitly if it stays only in a steady state. A pulse load applied to a fatigue crack propagating under constant amplitude loading induces a disturbance in the subsequent crack growth behavior and the analysis of the associated transient process would be useful to understand the fundamental mechanism operating in the tip of the advancing crack. In the case, after the application of a single overload, the crack continues to extend at a decreasing rate until an inflection point of the minimum growth rate is reached (delayed retardation; Fig.1). Then the crack propagates at an increasing rate it recovers its original growth rate. The overload affects the crack in

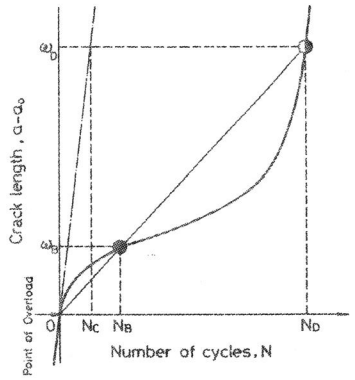

Fig.1. Schematic illustration of delayed retardation phenomenon [2].

two different ways, resulting in different crack closure behaviors [1]. The residual plastic strain left by overload tends to close the crack tip. This closing force is expected to be maximum just after the application of the peak load and decreases as the increasing distance from the point of overload. On the other hand, the geometric blunting of the crack tip due to the application of the overload tends to open up the crack tip and cancel the closing force due to the residual strain. Thus the effect of blunting delays the occurrence of the maximum retardation up to the inflection point (at $a - a_0 = \omega_B$ and $N = N_B$ in Fig.1).

On the basis of the crack closure conception proposed by Elber [11], the subsequent crack growth rate after the application of a single overload, $(da/dN)_D$, was described by

$$(da/dN)_D = C_0(U_D\Delta K)^m = U_D^m(da/dN)_C, \qquad (1)$$

where $(da/dN)_C = C_0\Delta K^m$ is the crack growth rate under constant amplitude loading and U_D is the crack opening parameter during the retardation, being a function of ω_B/ω_D and the current crack distance, $a - a_0$ [2]. When the ratio of peak stress range to baseline stress range is equal to 2, the crack growth rate at the inflection point, $(da/dN)_B$, is simply given by

$$(da/dN)_B = (\omega_B/\omega_D)^m(da/dN)_C. \qquad (2)$$

EXPERIMENTAL RESULTS

The material tested were five steels, two aluminum alloys and one titanium alloy. Their chemical compositions and heat-treatments are given

Table 1. Mechanical properties and material parameters

Material	Yield stress σ_y (MPa)	U.T.S.	Elongation (%)	Young's modulus E (GPa)	Poisson's ratio ν	Burger's vector b (nm)
HT80 steel	823	882	32	206	0.28	0.248
SNCM8 steel	942	1062	18	206	0.28	0.248
A553 steel	698	745	37	206	0.28	0.248
SUS304 steel	336	633	60	206	0.28	0.248
SS41 steel	270	441	33	206	0.28	0.248
A5083-O Al	148	329	20	70	0.34	0.286
A2017-T3 Al	322	446	23	70	0.34	0.286
Ti-6Al-4V	980	1050	16	117	0.34	0.295

in a previous paper [3]. The mechanical properties are listed in Table 1. Most of the crack growth tests were carried out in the intermediate crack growth rate region under zero-to-tension loading on center-cracked specimens, while some were on CT specimens. The thicknesses of the specimens were varied widely between 2 and 30mm. The peak/baseline stress ratio was maintained at 2.

The solid curves in Fig.2 represent $(da/dN)_C$ against ΔK for various materials. The $\log(da/dN)_C$ vs $\log\Delta K$ relationships for steels and titanium alloy appeared almost linear in the range of testing, while those for the aluminum alloys became convex upward. The overload tests were performed at the respective points symbolized differently among the materials. The results of the overload tests are summarized in Figs.2 and 3. Figure 2 shows the values of $(da/dN)_B$ together with those of $(da/dN)_C$. Figure 3 shows ω_B/ω_0 and ω_D/ω_0 against ω_0/B, where B is the specimen thickness and ω_0 is the monotonic plastic zone size at the baseline stress intensity range, being obtained according to the Dugdale model for small scale yielding as $(\pi/8)(\Delta K/\sigma_y)^2$ (σ_y: the monotonic yield stress). It is evident in Fig.2 that the $(da/dN)_B$ values disperse by a factor of 200, while the $(da/dN)_C$ range a factor of 50. The retardation was particularly strong in A5083 Al alloy, and the others seem to have a similar tendency. Thus the results of A5083 Al alloy are discussed in comparison with those of HT 80 steel, the most standard material.

The $(da/dN)_B$ values of both the materials dispersed significantly

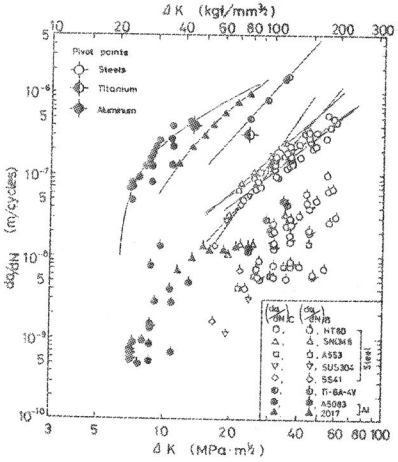

Fig.2. $(da/dN)_C$ and $(da/dN)_B$ against ΔK.

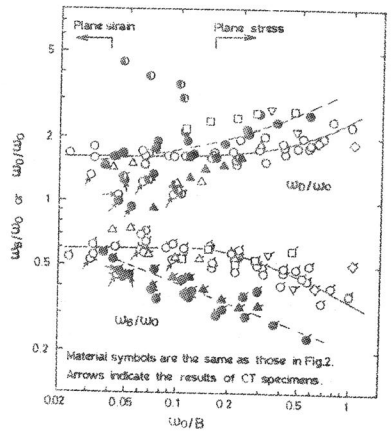

Fig.3. ω_D/ω_0 and ω_B/ω_0 against ΔK.

even at an equal ΔK level. This is because ω_B and ω_D were dependent on the overloaded states at the crack tip. Figure 3 demeonstrates that both the values varied with ω_0/B as indicated by the dashed and solid curves, respectively, for the two materials. ω_D/ω_0 tended to increase as the increase in ω_0/B, while the converse was seen for the data of ω_B/ω_0. This suggests that the effect of the residual plastic strain left by overload became stronger relative to the effect of geometric blunting of the crack tip as the stress states approached plane stress. However, the tendency appeared somewhat different between the two materials. Both ω_D/ω_0 and ω_B/ω_0 values in HT80 steel became almost constant as the plane strain condition was satisfied, whereas those in A5083 Al alloy varied depending on ω_0/B in the whole test range. This will be implicitly related to the different behaviors in the crack growth rate under constant amplitude loading in Fig.2 between the two materials. Namely, HT80 steel had a linear $\log(da/dN)_C$-$\log\Delta K$ relationship with a slope m approximately equal to 2, while A5083 Al alloy had a non-linear one with m varying with ΔK. Finally it is noted that CT specimens of A5083 Al alloy and HT80 steel (arrow marks) gave much smaller ω_D/ω_0 values compared with center-cracked specimens. Moreover, it is also remarked that the titanium gave anomalous values in both ω_D/ω_0 and ω_B/ω_0. This was due to the occurrence of cleavage

fracture at the overload in the center part of specimens.

NON-DIMENSIONAL EXPRESSION OF CRACK GROWTH RATE

It is pointed out [9, 10] that $\log(da/dN)_C$ vs $\log\Delta K$ curves pass a pivot point charcteristic of the material. The pivot points for steels, aluminum alloys and titanium alloys [9] are indicated in Fig.2. These become almsot coincident in a non-dimensional coordinate system as shown in Fig.4. Here the ordinate is normalized by Burger's vector b and the abscissa is described by the normalized cyclic J-integral $\Delta J/2\gamma$. The ΔJ values are evaluated by $(1 - \nu^2)\Delta K^2/E$ and the surface energy γ by Eb/20, where E is the young's modulus and ν is the Poisson's ratio. The material parameters used in the calculation are listed in Table 1. The results for the overload tests in Fig.2 are rewritten in Fig.4 together with those for constant amplitude loading. The former are shown by tailed marks as the relationship between $(da/dN)_B$ and the effective ΔK ($= U_D\Delta K = (\omega_B/\omega_D)\Delta K$). It is obvious that both the results for all the materials tested were nearly coincident by the generalization. Furthermore, it is interesting that the results in the steels fell along the solid line with a slope of one in the log-log scale. That is, $(da/dN)/b$ was linearly correlated with $\Delta J/2\gamma$ for the steels, while the relationship for the aluminum

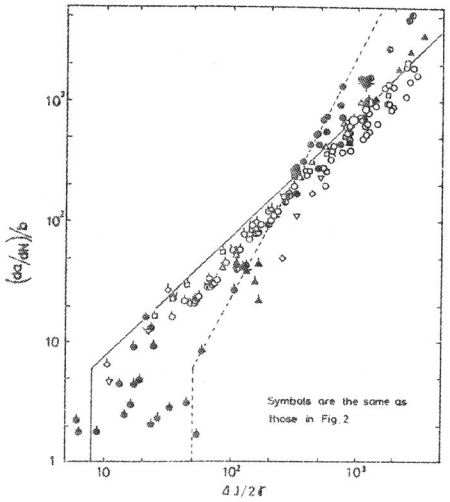

Fig.4. Non-dimensional expression of crack growth rate.

alloys appeared rather complicated. This implies that the cracks in the steels propagate in a stable manner satisfying the energy criterion suggested by Tanaka [10], whereas those in the aluminum alloys do so in an unstable manner depending on the applied ΔK level.

REFERENCES

[1]. Matsuoka, S., Tanaka, K., and Kawahara, M., The Retardation Phenomenon of Fatgiue Crack Growth in HT80 Steel, Engng Fract, Mech., 8 (1976), 507.

[2]. Matsuoka, S. and Tanaka, K., Delayed Retardation Phenomenon of Fatigue Crack Growth Resulting From a Single Application of Overload, Engng Fract. Mech., 10(1978), 515.

[3]. Matsuoka. S., and Tanaka, K., Delayed Retardation Phenomena of Fatigue Crack Growth in Various Steels and Alloys, J. Mat. Sci., 13 (1968), 1335.

[4]. Matsuoka, S. and Tanaka, K., Influence of Stress Ratio at Baseline Loading on Delayed Retardation Phenomena of Fatigue Crack Growth in A553 Steel and 5083 Aluminum Alloy, Eng. Fract. Mech.,11(1979), 703.

[5]. Matsuoka, S. and Tanaka, K., The Influence of Sheet Thickness on Delayed Retardation Phenomena in Fatigue Crack Growth in HT80 Steel and A5083 Aluminum Alloy, Eng. Fract. Mech., 13(1980), 293.

[6]. Tanaka, K., Matsuoka, S., Schmidt, V. and Kuna, M., Influence of Specimen Geometry on Delayed Retardation Phenomena of Fatgiue Crack Growth in HT80 Steel and A5083 Aluminum Alloy, "Advances in Fracture Research" edited by D. Francois et al., Pergamon Press, (1981), 1789.

[7]. Rice, J. R., Mathematical Analysis in the Mechanics of Fracture, "Fracture", edited by H. Liebowitz, Academic Press, II(1968), 191.

[8]. Dowling, N. E., and Begley, J. A., Fatigue Crack Growth During Gross Plasticity and the J-Integral, ASTM STP590, (1976), 82.

[9]. Tanaka, K., Masuda, C., and Nishijima, S., The Generalized Relationship Between the Parameters C and m of Paris's Law for Fatgiue Crack Growth, Scripta Met., 15(1981), 259.

[10]. Tanaka, K., The Cyclic J-Integral as a Criterion for Fatigue Crack Growth, Int. J., Fracture, in press.

[11]. Elber, E., The Significance of Fatgiue Crack Closure, ASTM STP486, (1971), 230.